AIAA JOURNAL
Vol. 41, No. 4, April 2003

Lessons from LESFOIL Project on Large-Eddy Simulation of Flow Around an Airfoil

Christopher P. Mellen,* Jochen Fröhlich,† and Wolfgang Rodi‡
University of Karlsruhe, 76128 Karlsruhe, Germany

A synopsis of important results obtained by seven partners in the Brite–Euram project LESFOIL sponsored by the European Union is presented. This project was devoted to assessing the feasibility of large-eddy simulations (LES) for the computation of the flow around an airfoil. As a test case, the Aerospatiale A-airfoil at $Re = 2 \times 10^6$ and 13.3-deg angle of attack was chosen. All partners performed simulations of this flow with various methods, most of which employed finite volume schemes and various subgrid-scale models of eddy-viscosity type. The key results of the individual partners' publications are presented in a comparative way. It is demonstrated that this configuration with realistic conditions for aeronautical flows is extremely demanding for LES. One reason is the need to achieve a threshold resolution for the adequate discretization of the attached and mildly separating boundary layer. The second and even more demanding requirement is the need for an adequate treatment of transition, which in the present computations was achieved by increased resolution.

Nomenclature

C	=	Courant–Friedrichs–Lewy number
C_D	=	drag coefficient (average value)
C_f	=	local friction coefficient (average value)
C_L	=	lift coefficient (average value)
C_p	=	local pressure coefficient (average value)
c	=	chord length of the profile
f	=	frequency
N_x, N_y, N_z	=	computational cells in streamwise, wall-normal and spanwise directions (C grids)
Re_c	=	Reynolds number, $U_\infty c/\nu$
Sr	=	Strouhal number
t_a	=	averaging time
U_∞	=	freestream velocity
u, v	=	components of instantaneous resolved velocity in tangential and wall-normal directions, respectively
u', v'	=	fluctuating components of velocity, for example, u' equals $u - \langle u \rangle$
x	=	coordinate along cord of airfoil
y	=	coordinate perpendicular to wall
y^+	=	wall distance in wall units
z	=	spanwise coordinate
α	=	angle of attack
Δ	=	measure for step size of the computational grid in space
Δ_t	=	time step
Δ_x, Δ_y, Δ_z	=	step size of the grid in x, y, and z directions, respectively
δ	=	boundary-layer thickness
ν	=	kinematic viscosity
$\langle\ \rangle$	=	spatial and temporal averaging

Received 27 November 2001; presented as Paper 2002-0111 at the 40th Aerospace Sciences Meeting, Reno, NV, 14–17 January 2002; revision received 23 September 2002; accepted for publication 23 September 2002.

*Postdoctoral Researcher, Institute for Hydromechanics.
†Postdoctoral Researcher, Institute for Hydromechanics. Member AIAA.
‡Professor, Institute for Hydromechanics. Associate Fellow AIAA.

Introduction

LARGE-EDDY simulations (LES) are used increasingly to solve flow problems that prove to be difficult to tackle with statistical [Reynolds averaged Navier–Stokes (RANS)] turbulence models. Among these flows are those exhibiting vortex shedding and massive separation. The aeronautical community has in recent years shown increasing interest in exploiting the capabilities of LES, especially with regard to providing information on acoustic phenomena or on the unsteady forces acting on a system. However, LES at the Reynolds numbers typically encountered in aeronautical applications poses formidable challenges. Indeed initial application of the LES approach to such flows met with considerable difficulties related to the generation of wiggles in the nose region,[1] to the treatment of transition,[2] and to the width of the computational domain.[3] Against this background, the European research project LESFOIL was initiated in 1997 with the prime aim to assess the feasibility of LES for calculating the flow around airfoils in a joint effort of partners from various European countries.[4] The research consortium consisted of Alenia Company, Italy; Chalmers University, Sweden (coordinator); CERFACS, France; Dassault Aviation, France; FLUENT Europe, United Kingdom; Institute for Hydromechanics (IFH), University of Karlsruhe, Germany; ONERA, France; University of Surrey, United Kingdom; and University of Manchester (UMIST), United Kingdom. [During the project, the investigators moved to Queen Mary and Westfield College (QMW), London.] Work in the project was started in various tasks dealing with subgrid-scale modeling, near-wall modeling, transition modeling, and numerical methods, which then fed in results to the final task of calculating the flow around an airfoil. The project is now completed, and details of the airfoil calculations performed by the various groups are and will be published in individual papers, for example, Refs. 5–7. A forthcoming book publication[8] will assemble the results from the entire project. Within the project, the IFH group at the University of Karlsruhe had the task of comparing and assessing the final LES airfoil calculations obtained by the various partners, and it is the purpose of the present paper to make these synoptic findings available to the aeronautical community.

Test Case Description and RANS Efforts

The configuration chosen as the test case for the LES airfoil calculations was the Aerospatiale A-airfoil at an angle of attack $\alpha = 13.3$ deg, the maximum lift configuration, and at a Reynolds number $Re_c = U_\infty c/\nu = 2.1 \times 10^6$, where U_∞ is the freestream velocity, c the chord length, and ν the kinematic viscosity. Such conditions are fairly realistic for aeronautical flows and constitute an extreme challenge for LES. This particular case was chosen because of the availability of experimental results and also because it

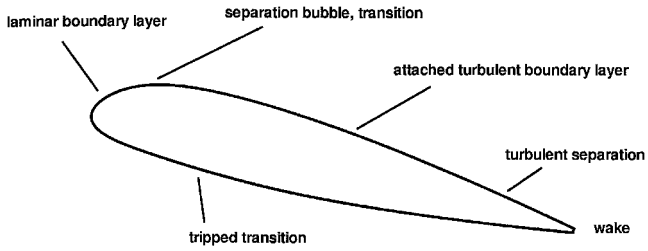

Fig. 1 Airfoil geometry and flow regions.

has been calculated already extensively using RANS models during the two previous European projects, EUROVAL[9] and ECARP.[10] The geometrical data of the profile are available on CD-ROM distributed together with Ref. 9. An overall impression of the flow phenomena involved is given in Fig 1. Along the upper (suction) surface the laminar boundary layer undergoes free transition in a small laminar separation bubble with turbulent reattachment at about $x/c = 0.12$. The turbulent boundary layer grows until it separates at $x/c = 0.83$, creating a small recirculation zone that extends to the trailing edge. The reverse-flow region extends to about $y/c = 0.016$ from the wall, whereas the point of maximum backflow occurs at $y/c = 0.003$. In the experiments, the transition on the lower (pressure) side was tripped at $x/c = 0.3$. The experimental data have been collected in two different wind tunnels, F1 (Ref. 11) and F2 (Ref. 12). In the F1 experiment, the lift and drag coefficients have been measured, as well as the friction coefficient C_f. These were also determined in the F2 experiment, supplemented by profiles of velocity and Reynolds stresses at several locations $x/c \geq 0.3$, that is, beyond transition. F1 furnished data for the pressure distribution, but no velocity data were collected. This is somewhat unfortunate because the drag coefficient differs between F1 and F2. To account for wall effects, the experimental angle of $\alpha = 13$ deg was corrected to $\alpha = 13.3$ deg as proposed in Ref. 13 and already employed for the computations within the ECARP project.[10]

The separation at the trailing edge acts to alter the airfoil's circulation from that of the inviscid case, also making a significant contribution to the drag. This point was highlighted in the previous European projects, where, unless the trailing-edge separation was well captured, global flow quantities such as lift and drag coefficients, C_L and C_D, matched the experimental values only poorly. What makes this test case so demanding is the high physical sensitivity of this slightly separating flow to details of the flow development. Consequently, the simulation is also very sensitive to the parameters and details of the computation. This flow is much more difficult to predict than a situation involving massive separation at high angles of attack or where separation occurs at an almost sharp edge.[14]

The RANS computations within the framework of ECARP[10] were performed with a large variety of different models ranging from algebraic models to Reynolds stress models (RSM). It turned out that in some cases fairly good results can be achieved, even with relatively simple models, such as the Johnson–King model, whereas standard RSM and most two-equation models failed. Only modified versions of these models, for example, reducing anisotropy and consequently the near-wall stress by truncating the RSM, yield realistic separation behavior, similar to nonlinear eddy-viscosity models. According to Haase et al.,[10,11] a drawback of these corrections is that they are not based on well-understood physical considerations." With LES, the amount of modeling is substantially reduced and traded against grid points and computation time. The motivation for the LESFOIL project, therefore, was to investigate whether such flows can be computed successfully with LES and at which computational cost.

Details of Various Computations

The primary objective of the project was to assess the feasibility of using LES to calculate the flow around single-element airfoils. A number of additional objectives or tasks were also pursued over the course of the project. These were to develop and evaluate subgrid-scale models applicable to real, industrial flows; to develop highly efficient numerical methods for the LES of airfoil flows; to develop and evaluate near-wall models based on the eddy-viscosity concept; and to develop and evaluate means of modeling the transition that occurs on the suction side of an airfoil. Many of these tasks were framed in the knowledge that controlling the potential cost of the airfoil calculations would overall be one of the most challenging aspects of the project. Thus, it was hoped that positive outcomes from each of these tasks would, when applied in unison, permit high quality LES results to be obtained using relatively coarse meshes with low to moderate computational requirements.

Over the course of the project, some partners tested many different combinations of parameters, models, and numerical procedures. Issues such as the grid resolution and the spanwise extent of the calculation domain were also addressed so that by the time of the project's completion a large body of experience and technical knowledge had been collected. For reasons of brevity, this paper reports only on what is considered to be each partner's most successful computation. The methods and parameters employed in these simulations are comprehensively summarized in Table 1. In the present paper, we can of course describe the different methods only in as much as is relevant for the subsequent discussion. For more details and further simulations with different parameters and methods see the individual partner's publications.

Table 1 lists the subgrid-scale models, near-wall models, convection schemes, and mesh sizes used. An appreciation of these simulation details is important for the discussion that follows, and hence, they will be discussed at some length in the next sections. Because numerical methods also strongly influenced the direction of the project, it will also be discussed at this point.

Mesh Resolution and Near-Wall Modeling

Mesh generation remained an important topic for the entire duration of the project. With LES, the mesh generally acts as an implicit filter applied to the motions of different length scales in the flow. Fluid motions smaller than the filter width must be accounted for by an appropriate subgrid-scale model. If the mesh does not resolve adequately the near-wall regions of the flow, additional modeling is required so that the wall shear stress is properly represented. Of course, the coarser the mesh, the more emphasis is placed on the subgrid-scale and near-wall modeling.

Initial airfoil computations were undertaken by all partners using fairly coarse meshes. Measured in wall units, the streamwise resolution of these grids was typically $\Delta_x^+ = 1000 \sim 2000$, due primarily to the extremely high Reynolds number of the flow. Usually, an LES computation with wall modeling should employ a grid with $\Delta_x^+ \lesssim 400$. These values can also be related to the boundary-layer thickness, which, for example, at $x/c = 0.5$ is around $\delta^+ = 2000$ in wall units. This explains why the results obtained with such coarse meshes were uniformly unsatisfactory. The length scales they resolved were simply not sufficient for correct functioning of the subgrid-scale and near-wall models employed. Consequently, most partners then embarked on a program of successive mesh refinement.

The computations represented in Table 1 have generally been undertaken on the finest mesh that each partner could afford. Some partners have used meshes of their own making. Others have used one of the so-called "common meshes" that were generated in the course of the project and distributed to the partners as a platform for the direct comparison of results.

The number of computational cells in each mesh is indicated by N_x, N_y, and N_z; the resolution in terms of wall units is Δ_x^+, Δ_y^+, and Δ_z^+. The numerical values reported for these are the maxima occurring after transition and are meant to convey the general order of magnitude rather than precise values. This information also reflects different modeling choices. At ONERA, for example, the near-wall region of the flow, was fully resolved and no wall model was employed at the price of a very fine grid close to the airfoil surface. All other partners used a coarser, sometimes even substantially coarser, grid together with some wall modeling approach. In most cases, this consisted of a wall function as indicated in Table 1. The Werner–Wengle model[15] (WW), a two- or three-part linear-logarithmic law (WL), or the no-slip condition (NS) was used. At FLUENT, the detached-eddy simulation (DES) approach[14] was employed, a method intended to perform well using resolutions much coarser in the wall-parallel directions than those typically associated

Table 1 Parameters employed by the different partners for their best simulations

Partner	Name of run	Equation solution	Mesh	Wall	Edge	L_z/c	N_x	N_y	N_z	Δ_x^+	Δ_y^+	Δ_z^+	Transition	Convection scheme	SGS	$\Delta_t U/c$	CFL	$t_a U/c$
CERFACS	Simu 2	Compressible flow	ONERA	WW	Sharp	0.02	256	64	18	1500	100	200	Triggered by white noise	Jameson + WD	WALE	2.96×10^{-6}	0.6	10
Chalmers	Smag 3	Incompressible flow	Chalmers	WL	Sharp	0.08	720	65	32	550	50	350	Blended van Leer	Central	SM	3×10^{-4}	1	>5
Dassault	Dassault	Compressible flow	Common unstructured wall function	WL	Blunt	0.036	8409		25	——	100	——	No particular measure	Stabil. SUPG	Selective SM	——	——	6
FLUENT	DES-3D	Incompressible flow	Common mesh B	DES	Sharp	0.03	360	64	16	1100	10	300	No particular measure	Central	SA-LES	3×10^{-4}	0.5	2
IFH	2D3D-3	Incompressible flow	IFH	WW	Blunt	0.06	2012	72	128	100	10	40	Blended upwind TS	Central	DSM	1×10^{-4}	0.65	>10
ONERA	M3	Compressible flow	ONERA	NS	Blunt	0.012	2760	90	72	60	2	25	Resolved	$AUSM^+(P)$ + WD	SMSM	3.3×10^{-5}	2	2.4
UMIST/ QMW	HD1	Incompressible flow	UMIST	WW	Sharp	0.12	768	128	64	500	20	200	No particular measure	Central	SM + VD	0.9×10^{-4}	0.2	5

with LES, and the choice of mesh reflects this fact. At another partner, Dassault, an unstructured mesh was used with 8409 unstructured points in 25 identical x–y planes.

Spanwise Extent of Calculation Domain

The spanwise extent L_z/c of the computational domain is an important issue because it places an upper limit on the size of the flow structures that may be represented. If this is chosen too small, it becomes difficult to ensure the physical realism of the computed flow.

Based on the estimated size of the likely flow structures in the trailing-edge separation, it was initially suggested that an acceptable minimum would be $L_z/c = 0.12$. This corresponds to about 1.5δ at the trailing edge (Fig. 2). The data in Table 1 show, however, that, except for one partner, an L_z/c smaller than this value was used. It was found that to match the computational resources to the original L_z/c specification would have allowed a mesh with a spanwise resolution Δ_z^+ only an order of magnitude greater than what is considered reasonable for an LES computation. Because an adequate spanwise resolution is one of the key requirements for the success of an LES, most partners reduced L_z/c, at the risk of altering to some extent the largest-scale features of the flow. The results will show that this turned out to be a successful compromise. Only in the computation with the smallest L_z/c (from ONERA, where $L_z/c = 0.012$ was used) was there evidence that the reduction in spanwise extent had influenced adversely the computed flow, and this only in the region downstream of $x/c \sim 0.8$.

Trailing-Edge Geometry

The test-case airfoil features a blunt trailing edge of approximately $h_e = 0.005c$ in height. This feature was not always represented in the computations, and in fact the previous RANS studies in Refs. 9 and 10 had all assumed a sharp trailing edge. In the geometry, taken over from Ref. 10 for the computations with a sharp edge, the upper surface was unchanged, and the lower surface adjusted smoothly starting from the location of maximum thickness at $x/c = 0.4$. To appreciate the impact of the blunt edge, its height has to be compared to the thickness of the reverse-flow region of $0.016c$ and to the boundary-layer thickness at the edge of about $0.1c$, as shown in Fig. 2. During the project, Mary and Sagaut performed companion simulations with $N_z = 30$, both with a sharp edge and with the blunt edge, while keeping all other parameters unchanged (private communication, 2001). They detected no change in the flow statistics due to the change in geometry. Other partners undertook similar but more qualitative comparisons and reached basically the same conclusion. Thus, it was concluded that the presence or absence of the blunt trailing edge had little impact on the computational results in the case considered.

CFL Number and Integration Time

The unsteady motion resolved in space by an LES computation also needs to be resolved in time. Hence, for physical reasons, the local Courant–Friedrichs–Lewy (CFL) number $C = \Delta_t |u|/\Delta$ must be kept at a magnitude of order unity, even when implicit time integration is employed. (Here $|u|$ is the magnitude of the velocity vector, and Δ represents the mesh size of the grid.) In Ref. 16, a related study was undertaken that yielded significant changes in the results only for increasing C beyond 3 in a direct numerical simulation (DNS). Table 1 shows that this requirement was met.

Extraction of accurate statistical quantities from an LES requires averaging of the unsteady computation over an integration time that far exceeds the characteristic time of the predominant flow features. Because of computational constraints, not all partners were able to perform long-time averaging. However, the results from those computations with shorter integration times do not show any identifiable adverse effects. When the C_L and C_D time histories of their computations were examined, some partners observed that these coefficients oscillated with a Strouhal number $Sr = fc/U_\infty$ of approximately 10, where f is the dominant frequency of the signal. This explains why relatively small values of $t_a U_\infty/c$ apparently did not affect the statistics obtained. However, in the highly resolved computations of ONERA and IFH, the observed Strouhal numbers were about 1.3 and 1.4, respectively.

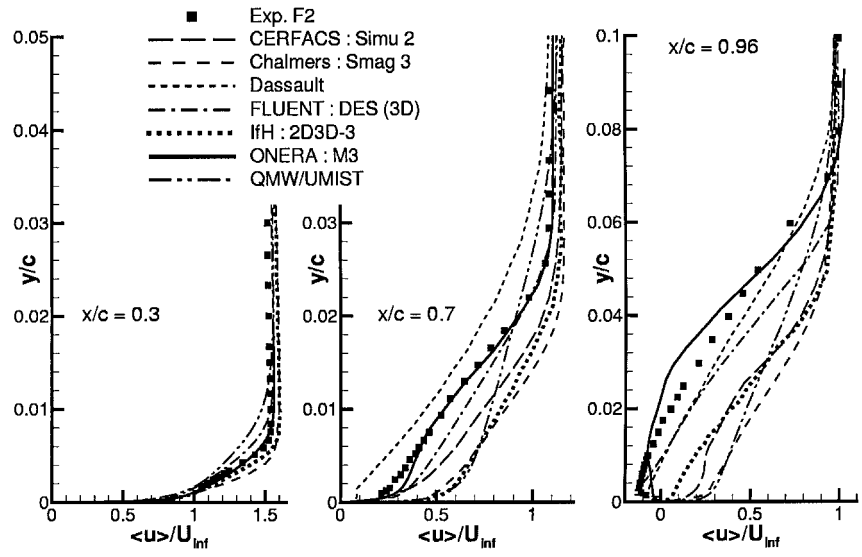

Fig. 2 Profiles of average velocity $\langle u \rangle / U_\infty$.

Convection Scheme and Subgrid-Scale Model

The subgrid-scale (SGS) models used by the different partners in the computations presented here encompass different eddy-viscosity models such as the Smagorinsky model (SM), its selective as well as its dynamic variant (DSM),[17,18] the WALE model,[19] and the selective mixed scale model (SMSM).[20] The DES approach[14] also employs an eddy-viscosity SGS model, the LES variant of the Spalart–Allmaras model.[21] At UMIST/QMW, the SM was employed with van Driest damping (VD), whereas at Chalmers it was not.

The solution codes of most partners used various second-order centered schemes when discretizing the convective fluxes. Such choices are very common in practical applications of the LES method. Unfortunately, flows computed with centered convection schemes and meshes of large cell Reynolds number (here defined using the effective viscosity) are prone to exhibiting numerical "wiggles" in the resolved velocity and pressure fields. This problem was encountered by all partners, and the typical response was to add some form of selective upwind bias to the convection term. Further details are given in a later section on transition modeling.

Numerical Methods

At the start of the project, all partners had in their possession a parallelized solver code. Parallelization was generally achieved via the domain decomposition approach, using the message passing interface (MPI) or the parallel virtual machine (PVM) for the interdomain communication. At ONERA, CERFACS, and Dassault, codes were used that solved the compressible flow equations whereas all other partners applied incompressible methods. Dassault was also the only partner employing the finite element methodology. Finite volume discretization was used by all others.

During the course of the project, considerable effort was devoted toward optimization of the solution methods and toward methods for minimizing the computational requirements of the airfoil computations. Part of the work took advantage of the spanwise periodicity of the configuration by using a Fourier transform to convert the discrete three-dimensional pressure Poisson equation into a more easily solved set of two-dimensional equations. Where employed, significant speedup was achieved compared to more generalized algorithms such as, for example, a three-dimensional solver using the strongly implicit procedure (SIP).

At Chalmers and FLUENT, implicit time-integration algorithms were used. During the airfoil computations, studies were undertaken into the relative merits of different pressure-correction-based solution methods. The SIMPLE, SIMPLEC, and PISO schemes were evaluated. Ultimately in terms of the overall CPU time requirements, it was found that SIMPLEC and PISO were equally useful.

Toward the end of the project, a strategy of a two-dimensional/three-dimensional zonal mesh was introduced by ONERA, an approach which was then also adopted at IFH. This method takes

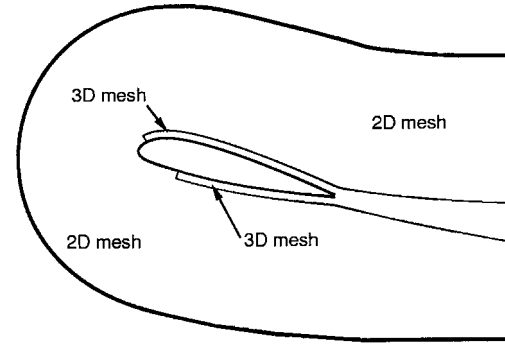

Fig. 3 IFH: two-dimensional/three-dimensional zonal mesh.

advantage of the fact that, outside the airfoil boundary layer, the flow is largely inviscid and two dimensional, whereas a fully three-dimensional mesh is only required in the turbulent boundary layer and the wake. Figure 3 illustrates the concept. Along the interface between the two zones, the discretization ensures conservation of mass and momentum fluxes. The two-dimensional mesh is naturally unable to support any turbulence and, hence, the interfaces between the two-dimensional and the three-dimensional mesh have to be situated in regions that contain two-dimensional laminar or inviscid flow. On the upper and lower surface, the three-dimensional mesh typically commences just upstream of the point of transition in the experiment ($x/c = 0.12$ on the upper surface and $x/c = 0.3$ on the lower surface). In the LES of ONERA, on the lower surface this was even shifted close to the trailing edge for cost reasons. Normal to the wall, the IFH three-dimensional mesh extended to about $0.23c$ from the wall in the rear part, which is about four times the boundary-layer thickness. In the computations undertaken with this strategy, approximately 50% of the grid points in the nominally three-dimensional mesh could be removed by replacing the three-dimensional grid by its two-dimensional equivalent. Correspondingly, the computation time required was reduced by nearly a factor of two.

Of considerable interest is the CPU time required by the various computations. Some examples are ONERA's M3 simulation required ~150 CPU h per integration time unit c/U_∞ on a single processor of a NEC SX5; Chalmer's Smag 3 computation required totally ~180 CPU h per time unit when running on 32 processors of an IBM RS/6000 SP; due to the much finer grid used, the IFH computation needed ~1800 CPU h per time unit on 52 processors of an IBM RS/6000 SP2. The range of hardware that was employed across the project makes objective comparisons of CPU requirements somewhat difficult. However, the figures given are sufficient to indicate that large computational resources are required.

Discussion of Results

Figures 2 and 4–9 present comparative plots of the results. Because the critical part of the flow is on the suction side and profiles have been measured only there, the discussion is focused on this side of the profile. There, the flow separates from the airfoil surface at $x/c = 0.83$, and capturing the subsequent small trailing-edge separation zone makes this flow a particularly difficult case for calculations. The development of the mean velocity profiles is shown in Fig. 2 at three axial stations. At the earliest station ($x/c = 0.3$), all predicted profiles are still reasonably close to the experiments, but already here the ONERA calculations show the best agreement. This continues farther downstream. At $x/c = 0.7$, the flow approaches separation, and there are already significant differences between the various calculations. In the results of ONERA, the velocity profile is captured very well. In those of FLUENT, also the approach to separation is produced, whereas in the Dassault predictions, this is somewhat too fast. The other calculations show little tendency toward separation. At $x/c = 0.96$, the region with negative velocity has a thickness of about $0.016c$. The ONERA results are still closest to the measurements, but now there are more significant deviations. The results of Dassault and FLUENT also show a separation region that is, however, considerably smaller than the measured one. All of the other calculations do not predict separation, and the profiles are, therefore, much too full at this location. The IFH results show some tendency toward separation, and it is somewhat surprising that separation is not produced in view of the fairly well-predicted turbulence quantities as will be discussed.

At the same streamwise locations, the profiles of the resolved turbulent stresses $\langle u'u' \rangle$, $\langle v'v' \rangle$, and $\langle u'v' \rangle$ are compared with the measurements in Figs. 4, 5, and 6, respectively. (Results are not available from all of the partners and not always for all of the three stresses.) All partners had difficulties in predicting consistently the stresses. Before separation, at $x/c = 0.3$ and 0.7, the ONERA computation is generally in best agreement with experimental data and predicts the distribution of all three stresses reasonably well. (The simulation M3 reported here[6] has later been continued for another 2.4 time units resulting in an improvement of $\langle v'v' \rangle$ and $\langle u'v' \rangle$.[22]) However, once separation occurs, the limited spanwise extent of this computation ($L/z = 0.012c$ only) appears to become ill suited to the thickening boundary layer and the occurrence of a separation region, as reflected by the $\langle u'u' \rangle$ profile. This imposes unphysical constraints on the large-scale structures present in this region and causes the resolved stresses to differ from the experimental data, partly in level and partly in distribution. Although the average velocity is generally too high, the $\langle v'v' \rangle$ and $\langle u'v' \rangle$ fluctuations predicted by the IFH computations are fairly realistic at $x/c = 0.3$ and 0.7 and near the wall also at $x/c = 0.96$. It is, however, noticeable that, as with most other partners, the streamwise fluctuations $\langle u'u' \rangle$ very

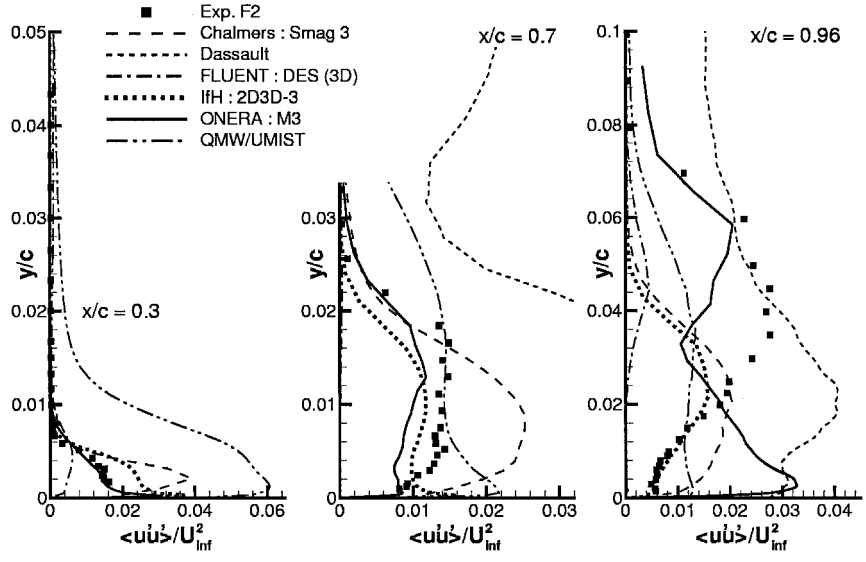

Fig. 4 Profiles: $\langle u'u' \rangle / U_\infty^2$.

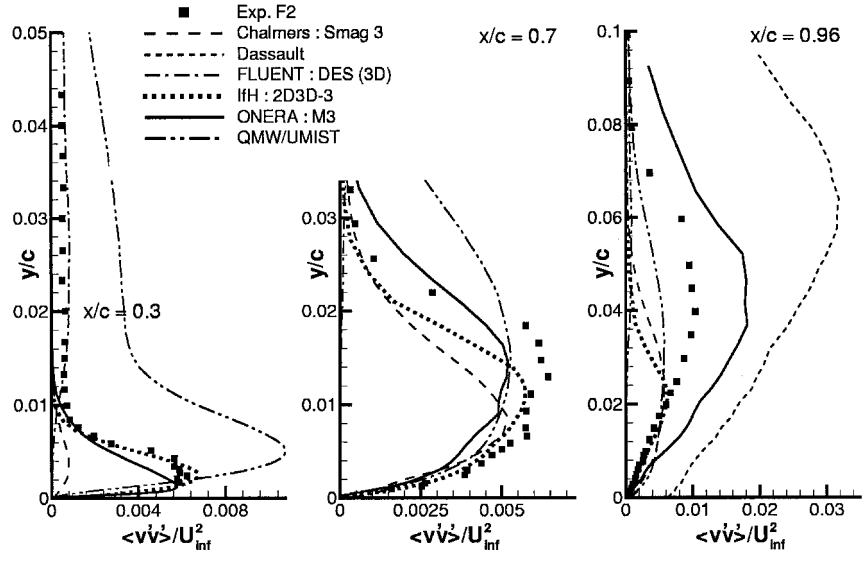

Fig. 5 Profiles: $\langle v'v' \rangle / U_\infty$.

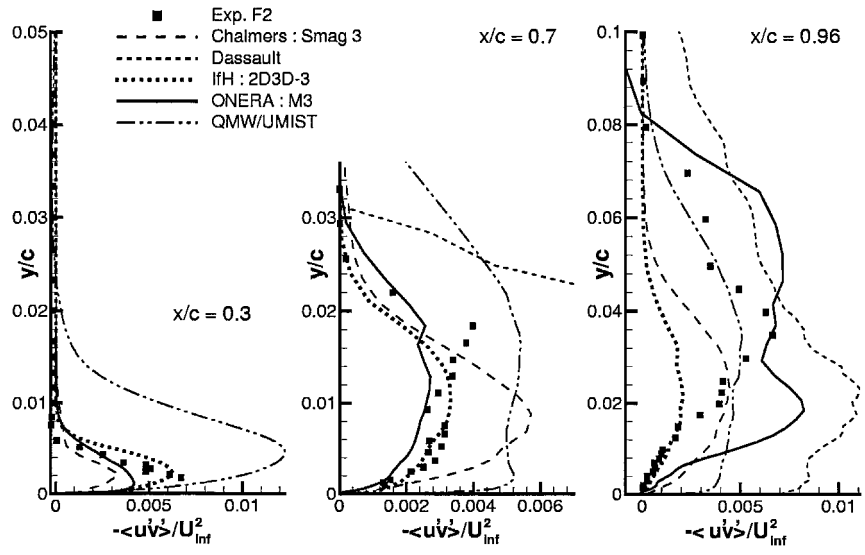

Fig. 6 Profiles: $\langle u'v' \rangle / U_\infty^2$.

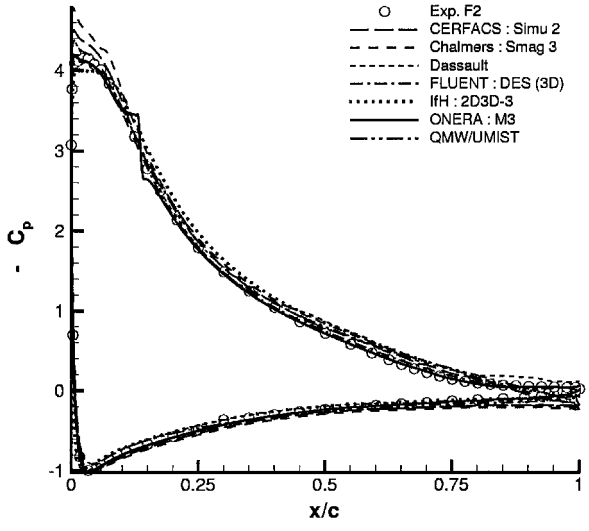

Fig. 7 Pressure coefficient.

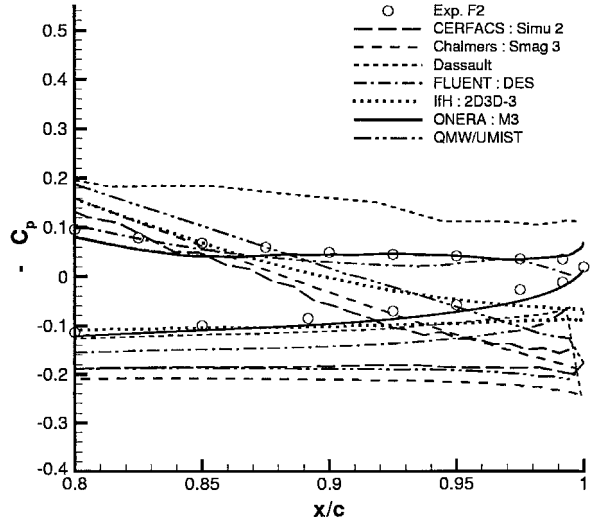

Fig. 8 Pressure coefficient near the trailing edge.

near the wall are significantly overpredicted at the earlier stations. This behavior is often seen in LES computations that underresolve the flow, and in channel flow, computations yield a velocity profile that is too full near the wall. At Dassault, far too large turbulent stresses are predicted, especially at $x/c = 0.7$, where they are an order of magnitude larger than in the experiment (in Fig. 5 outside the range shown). In view of this, it is somewhat surprising that their mean flowfield is reasonably well predicted. The DES calculation of FLUENT, on the other hand, yields stresses $\langle u'u' \rangle$ and $\langle v'v' \rangle$ at $x/c = 0.7$ and 0.9 ($\langle u'v' \rangle$ is not provided), which are much smaller than the measured ones. It appears that, due to the coarse grid, in these calculations the resolved fluctuations do not contribute much to the momentum exchange and that here it is mainly the model that contributes.

The distribution of the pressure on both the pressure and the suction side is shown in Fig. 7, with details near the trailing edge enlarged in Fig. 8. The ONERA and FLUENT DES computations best capture the global pressure distribution. This is consistent with a reasonably accurate representation of the trailing-edge separation. Note that the extremely fine resolution of the ONERA mesh made it possible to capture the small pressure plateau associated with the laminar separation that occurs at $L/c \approx 0.1$. This is a significant achievement, but at a considerable expense. The computations, which do not produce the trailing-edge separation, also fail to show the pressure plateau in this region and generally have at the leading edge a suction peak that is too large. Dassault attributes their rather high trailing-edge pressure plateau to their inability to capture the laminar separation bubble in the transition region, thereby altering the circulation and, hence, the pressure distribution.

The lift and drag coefficients are compiled in Table 2. Most calculations predict the lift coefficient C_L in reasonable agreement with both experiments. The CERFACS and Chalmers results are somewhat too high. It is unfortunate that the drag coefficient C_D measured in the two experiments is quite different; the FLUENT results agree very well with the F2 data, whereas the results of ONERA, IFH, and CERFACS fall in between the two measured values.

The distributions of the skin-friction factor C_f on the suction side are compared in Fig. 9. The experimental skin-friction distribution is matched very well by the results from the ONERA computation. It can be seen that the fine resolution of the mesh has enabled the capture of the reverse-flow region in the leading-edge laminar separation bubble. Of the other partners IFH achieves the best overall agreement with the experimental data at x/c upstream of 0.3, and their results also show the tendency to develop a laminar separation bubble. On the other hand, toward the trailing edge, FLUENT has the best agreement, but the calculated C_f distribution near the leading edge is certainly not realistic. Overall, it is obvious that the failure to predict the trailing-edge separation leads to C_f values near the trailing edge that are much too large.

It is also worth observing that all of the computations indicating separation at the trailing edge may be characterized by their use of comparatively small spanwise extents for the computational

Table 2 Comparisons of C_L and C_D

Partner	Run	C_L	C_D
CERFACS	Simu 2	1.655	0.0220
Chalmers	Smag 3	1.72	0.0170
FLUENT	DES-3D	1.568	0.0303
IFH	2D3D-1	1.54	0.0230
ONERA	M3	1.539	0.0250
UMIST/QMW	HD 1	1.553	0.0437
Experiment F1[11]	——	1.56	0.0204
Experiment F2[12]	——	1.515	0.0308

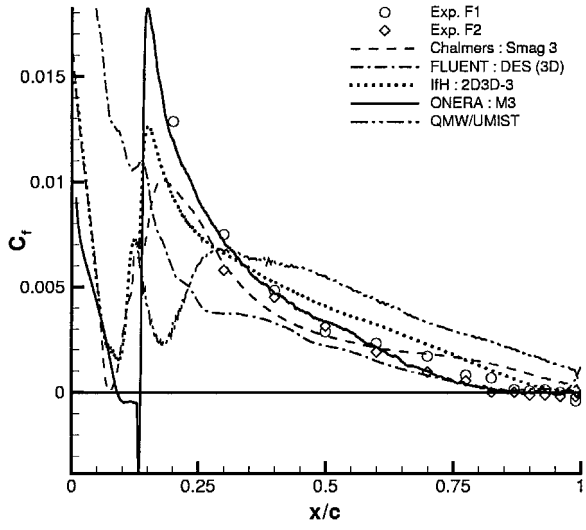

Fig. 9 Friction coefficient on the suction side.

domains. On one hand, the limited spanwise extent makes it possible to employ an increased spanwise resolution, that is, small Δ_z^+ as apparent from Table 1. As discussed earlier this is required to represent realistically the near-wall turbulent structures. Also, if wall function meshes are used, experience shows that good LES results are generally not achieved with $\Delta_z^+ \gg \Delta_y^+$ but require these to be roughly equal. In the present situation where transition occurs without an adequate transition model being available, this issue is even more pressing. On the other hand, the small domain size in some computations imposes restrictions on the large vortical structures. It suppresses three-dimensional effects of size equal or larger than the domain size and renders the flow more two dimensional, which applies in particular to the vicinity of the trailing edge. It is generally observed that, with increasing two dimensionality of the flow, the tendency toward separation increases. This effect might push the coarse grid results toward the experimental curves, for different reasons though than the highly resolved one. ONERA, for example, states that their result is influenced by this effect beyond $x/c = 0.8$. A quantitative assessment of the issue is possible by using a wide domain and computing the spanwise correlation. At Chalmers, such a study was performed with $L_z/c = 0.08$. The mesh employed was coarser than the one employed by ONERA, and no separation occurred. Because it is known that in the presence of separation the spanwise correlation increases, this yields a sort of lower bound on what would be expected with separation. Though not included in this paper, these results showed that at $x = 0.6c$ none of the velocity correlations vanishes beyond $dz/c = 0.012$ and that at $x = 0.9c$ zero crossings are located around $dz/c = 0.02$. However, the extent to which the results are influenced by this problem can not be quantified further because the results also depend on many other parameters such as grid resolution, grid stretching, etc. The main effect is that a reduced spanwise extent enhances the two dimensionality of the flow and produces a tendency to increased separation. This has been observed in Ref. 6, where the simulation M3 in Table 1 was repeated with a further reduction of L_z by a factor of two (at the same time reducing the number of points in this direction so as to maintain the effective resolution). This yielded an overprediction of both the size and strength of the recirculation region.

Lessons Learned from the Project

The preceding section presented and discussed each partner's best result. However, the airfoil computations undertaken over the duration of the project encompassed a range of solution parameters broader than seen here. In the following synthesis, the knowledge gained from these computations is also accounted for.

SGS Modeling

Generally it has been found that quantitative analysis of the merits of different SGS models in the context of airfoil flows is made difficult by the variety of parameters involved, such as grid resolution, transition modeling, and spanwise extent of the computational domain, which also influence the final result. However, qualitative inferences may be drawn.

On meshes that fail to resolve adequately the flow, no SGS model seems able to return satisfactory results. Generally this is characterized by an inability to predict the turbulent trailing-edge separation indicated by the experiments and also by often excessive velocity fluctuations in the near-wall region.

The most successful LES simulation, the ONERA M3 computation, also employed by far the finest mesh. However, only one SGS model was evaluated on this mesh. In related computations, this partner alternatively employed the monotonically integrated LES (MILES) approach instead of an explicit SGS model. MILES is based on the property of certain numerical schemes to introduce numerical dissipation that is then able to play a role similar to the dissipation introduced by an explicit SGS model. On a coarse mesh, the differences between the MILES approach and results from ONERA's explicit SGS model were found to be small.

The conclusion from the non-wall-resolving simulations performed for the airfoil configuration is that no clear advantage of one or another SGS model could be discerned. Rather, the overall results clearly indicated that the resolution of the chosen mesh has a much larger impact on the quality of the computations than the choice of SGS model.

Near-Wall Modeling

From the outset of the LESFOIL project, near-wall models were identified to be an important means of reducing the cost of the airfoil computations. The models used by each partner in their best computations are given in Table 1, and further models were also investigated in other computations.

The derivation of both the WW[15] and the WL models is based on the statistical properties of attached boundary layers. Interest in the LESFOIL project lay in observing the performance of this modeling for a boundary layer with a small separation region. Comparisons by partners on nominal wall-function meshes of each of these near-wall models to the situation where simply the no-slip boundary condition was applied indicated that both models generally improved predictions of quantities such as the skin-friction coefficient in the attached part of the boundary layer. Evaluation of their usefulness in the separated regions of the airfoil flow was, however, limited because in most of the partners' simulations, the boundary layer actually remained attached in the mean, although instantaneous intermittent reverse flow was observed in some of the computations.

This outcome should not necessarily be taken as an indication of the unsuitability of these approaches to regions of reverse flow as it is difficult to isolate the effect of any one parameter, such as SGS model, near-wall model, or mesh resolution, on the results of a computation. However, there is little doubt that the presence of the trailing-edge separation does pose certain challenges to the useful application of either of these models. For instance, it was recognized that in designing a wall-function mesh that is able to resolve adequately the region below the point of maximum backflow of the trailing-edge separation (a reasonable prerequisite) the distance of the first grid point from the wall y_1^+ of such a mesh is so small ($y_1^+ \leq 10$ in the turbulent boundary layer) that on application both the WW and the WL models virtually reduce to a no-slip condition.

In the results presented here, only at ONERA a mesh was used that fully resolved the near-wall region, that is, $y_1^+ = \mathcal{O}(1)$. Naturally, these conditions yield a marked increase in the cost of the computation compared to wall-function grids. Employing a substantially

coarser grid, the DES of FLUENT produced a mean flowfield matching the experimental data quite well. This approach uses a RANS turbulence model, here the Spalart–Allmaras (SA) ν_t model,[21] operating in unsteady mode, to represent the unresolved turbulent fluctuations close to the wall. In the interior of the flowfield this model is converted into a one-equation SGS model by replacing the wall distance as length scale by the cell size of the grid. The computations at FLUENT have been performed on a mesh with y^+ of the first grid point around 10. The originators acknowledge that the SA model would usually in fact require a wall-normal resolution of $y^+ = \mathcal{O}(1)$. Also, the spanwise resolution is very coarse (Table 1), and it is not clear from the results to which extent the computed solution is actually three dimensional. Therefore, it is not entirely clear why this DES calculation has been able to capture the trailing-edge separation while using a mesh much coarser than those of all other partners. However, as a result of the separation being obtained, the C_L and C_D determined by the DES simulation are quite satisfactory. It is unlikely, however, that this computation could be relied on to give accurate information on the structure of the turbulence. The resolved fluctuations are in fact smaller than the modeled ones, even in the outer flow near the trailing edge. According to the concept of DES, this would be the case only very close to the wall but not in a separated, detached flow.[23] Hence, it is felt that further studies are needed to investigate the sensitivity of DES to the various parameters involved. (See also discussion of Refs. 24–26 in the following.)

Transition Treatment

During the initial stages of the LESFOIL project, the approach was that a proper simulation of the transition mechanisms by LES could not be aimed for and that transition should be handled by special procedures with the aid of information from the experiments about the transition location. During the course of the airfoil computations, it became readily apparent that transition handling was very closely linked to the issue of numerical oscillations appearing in nominally laminar regions of the flow. These unphysical oscillations arose due to a combination of the high-Reynolds-number flow and the use of centered differencing schemes on relatively coarse meshes. They were suppressed by using one of the following two approaches: 1) explicit application of an upwind convection scheme and 2) use of a "wiggle detector" (WD), which added numerical dissipation when an unphysical oscillation was detected. This detector is active in all regions of the flowfield.

The partners employing the first approach (Chalmers, IFH, and UMIST/QMW) typically noted that, on coarse meshes once the calculations reverted to a centered convection scheme, the flow quickly became turbulent due to numerical noise arising from the discretization. This provided a means of a priori fixing the transition location. Usually a blending dependent on chord position was used to switch between the convection schemes gradually. In this manner, transition in the laminar separation bubble was not resolved, but the flow switched from a steady to a highly unsteady one by means of the numerically generated fluctuations. On the other hand, at IFH it was observed that on a fine grid this mechanism is insufficient to generate the required level of turbulence.[27] The introduction of a model transition strip (TS) was used as a remedy. Similar blendings as for the convection scheme were used in most computations to ensure that SGS models and turbulent wall functions only contributed to the nominally turbulent regions of the flow.

The second approach was employed at CERFACS and ONERA. When undertaking coarse-mesh computations it was recoginized at CERFACS that transition had to be promoted through the introduction of numerical forcing at a point near the prespecified transition location. At ONERA, however, it was found that, on the very fine mesh used in their calculation, numerical forcing was not needed. The resolution was in fact so good ($\Delta_y^+ \sim 2$, $\Delta_z^+ \sim 20$, and $\Delta_x^+ \sim 100$) that the actual transition processes was captured. In this calculation, a thin laminar separation bubble developed between $x/c = 0.09$ and 0.13; transition occurred in the free shear layer of this bubble followed by turbulent reattachment, and all of this agrees with observations from the experiments. Hence the location of transition was not fixed a priori, and this is in fact the only proper way to handle the transition process. However, it needs a very fine resolution, which could only be achieved by having a rather small spanwise extent of the calculation domain ($L_z/c = 0.012$).

The FLUENT DES calculation on a fairly coarse mesh also did not use an a priori specification of the transition location, but it is actually doubtful whether any transition occurred in this calculation. When the C_f distribution (Fig. 9), the straightforward application of the SA RANS model near the wall, and the employed near-wall resolution are examined, it is most likely that the boundary layer was turbulent right from the leading edge. Usually, achieving transition with the SA model (as with other RANS models) does require the use of a tripping mechanism.[27]

In suppressing unphysical oscillations, the use of a WD seems less ad hoc and more flexible than the explicit specification of regions in which an upwind convection scheme should be applied. This applies in particular to the situation with a fully three-dimensional geometry. Possible concerns about such a detector arise due to the difficulty in quantifying just when and where numerical dissipation is added. Furthermore, this term in fact acts as an additional subgrid-scale term. Traditionally, LES practitioners prefer to rely solely on SGS modeling for the turbulent energy drain.

Conclusions

The LESFOIL computations have brought significant advances in understanding the application of LES to airfoil flows at large Reynolds number and high angles of attack, which are characteristic for potential applications of the method under realistic aeronautical conditions. In turn the problems associated with such calculations have also become clear. In understanding these problems, the conclusion was reached that at present genuinely successful simulations of this type of flow can only be achieved by using a well-resolved LES in which near-wall turbulent structures are adequately resolved and transition is properly simulated. When these criteria are met, the results obtained are largely satisfactory. Although the computational demands of such calculations require compromises such as a reduced spanwise extent, the overall results obtained do not seem to be affected all that much, but further investigations are necessary. If these demands are not met, LES is not necessarily able to improve on RANS results. An example is reported in Ref. 24, where LES of the A airfoil is compared to the results obtained with the Baldwin–Lomax (BL) and the SA model showing no pronounced superiority of the LES. None of the three computations predicts separation, SA performing slightly better than BL in terms of mean velocity and fluctuations. On the other hand, using a substantially finer grid, Mary and Sagaut[6] found that LES predicts separation, whereas a computation with the SA model on the same grid (but two dimensional) does not. In a recent investigation after the termination of the LESFOIL project, Schmidt and Thiele[25] also performed a two-dimensional computation with the SA model, where they obtained separation near the trailing edge.

The combination of coarse grids with wall functions yielded results that are generally disappointing. It is now recognized that these computations were constrained in two important ways: the necessity to use ad hoc methods for treating the transition and the difficulties inherent in constructing a wall-function mesh with a y_1^+ value small enough to enable adequate resolution of the trailing-edge separation but yet large enough to permit the wall functions to be truly effective. These experiences have highlighted the importance of local mesh resolution. A possible remedy may be the use of locally refined unstructured or block-structured grids. The latter were employed by Schmidt and Thiele[26] in similar computations.

Altogether it was found that the resolution has the greatest influence on the calculations and is the key to success, whereas the SGS model appears to play a subordinate role.

The nominal resolution requirements of a DES are somewhat less stringent than those of LES, and for this reason DES appears to have some potential for successfully calculating the airfoil flows in question. Some further experience has been gained by Schmidt and Thiele,[26] who used DES to calculate the flow past a NACA 4412 airfoil with mild separation. In further computations performed in response to the results of the LESFOIL project, these authors recently computed the present A-airfoil configuration with their DES

method[25] employing the QUICK scheme for the convection term, which is known to introduce some numerical diffusion. The structured grid contained 440,000 points in total with $N_z = 20$ points over a spanwise extent of $L_z/c = 0.2$ yielding $\Delta_z^+ \leq 1678$. Two- and three-dimensional DES have been performed with very similar result. The trailing-edge separation was stronger than in the experiment, the fluctuations were smaller, and the Strouhal number was $Sr = 20$ in the three-dimensional case, whereas the flow was steady in the two-dimensional run and $Sr = \mathcal{O}(1)$ in the LES of ONERA and IFH discussed earlier. No refinement study was performed in this work. Hence, it is not certain that these DES really met the resolution requirements of the method.[23] With this in mind, no final conclusions can be drawn concerning the application of DES to the present configuration, and it is suggested that its testing should be pursued.

In summary it has been shown that, when known resolution requirements are met, LES is able to produce the correct overall flow behavior. This is achieved without the need for model tuning. Meeting these resolution requirements does, however, lead to calculations that are extremely expensive and, hence, currently not suitable for routine use. On the other hand, the returns from these computations are information rich because details are provided on the structure of the flow and its time-dependant behavior that are simply not available from RANS calculations. Furthermore, it can be expected that improved numerical techniques and ever increasing computer power will make such simulations more affordable in the future. Although such simulations with, for example, 100 million grid points can be undertaken at the time of writing, it seems questionable whether this strategy is the most cost-effective one. Hybrid LES-RANS methods of which DES is one variant might be better suited and should be developed further.

Acknowledgments

The first author was funded through the European Union project LESFOIL, BE97-4483. The second author was supported by the French–German program "Numerical Flow Simulation." Computation time for the authors' simulations was provided by the Computer Center Karlsruhe. The partners of the LESFOIL project are acknowledged for numerous stimulating discussions and for making their data available to the authors.

References

[1]Kaltenbach, H.-J., and Choi, H., "Large Eddy Simulation of the Flow Over an Airfoil on Structured Meshes," *Annual Research Briefs*, Center for Turbulence Research, Stanford Univ., Stanford, CA, 1995, pp. 51–60.

[2]Jansen, K., "Preliminary Large-Eddy Simulations of Flow Around a NACA 4412 Airfoil Using Unstructured Grids," *Annual Research Briefs*, Center for Turbulence Research, Stanford Univ., Stanford, CA, 1995, pp. 61–72.

[3]Jansen, K., "Large-Eddy Simulation of Flow Around a NACA 4412 Airfoil Using Unstructured Grids," *Annual Research Briefs*, Center for Turbulence Research, Stanford Univ., Stanford, CA, 1996, pp. 225–232.

[4]Davidson, L., "LESFOIL: A European Project on Large-Eddy Simulations Around a High-Lift Airfoil at High Reynolds Number," *Proceedings of ECCOMAS 2000* [CD ROM], Sept. 2000.

[5]Dahlström, S., and Davidson, L., "Large Eddy Simulations of the Flow Around an Aerospatiale A-Airfoil," *Proceedings of ECCOMAS 2000* [CD ROM], Sept. 2000.

[6]Mary, I., and Sagaut, P., "Large Eddy Simulation of Flow Around an Airfoil Near Stall," *AIAA Journal*, Vol. 40, No. 6, 2002, pp. 1139–1145.

[7]Cokljat, D., and Liu, F., "DES of Turbulent Flow Over an Airfoil at High Incidence," AIAA Paper 2002-0590, Jan. 2002.

[8]Davidson, L., Cokljat, D., Fröhlich, J., Leschziner, M., Mellen, C., and Rodi, W. (eds.), *LESFOIL: Large Eddy Simulation of Flow Around a High Lift Airfoil*, Springer, Berlin (to be published).

[9]Haase, W., Brandsma, F., Elsholz, E., Leschziner, M., and Schwamborn, D. (eds.), *EUROVAL: A European Initiative on Validation of CFD Codes*, Vol. 42, Notes on Numerical Fluid Mechanics, Vieweg, Brunswick, Germany, 1993.

[10]Haase, W., Chaput, E., Elsholz, E., Leschziner, M., and Müller, U. (eds.), *ECARP: Validation of CFD Codes and Assessment of Turbulence Models*, Vol. 58, Notes on Numerical Fluid Mechanics, Vieweg, Brunswick, Germany, 1996.

[11]Huddeville, R., Piccin, O., and Cassoudesalle, D., "Opération décrochage—mesurement de frottement sur profiles AS 239 et A 240 à la soufflerie F1 du CFM," ONERA, TR RT-OA 19/5025 (RT-DERAT 19/5025 DN), Paris, 1987.

[12]Gleyzes, C., "Opération décrochage—résultats de la 2ème campagne d'essais à F2—mésures de pression et vélocimétrie laser," ONERA, TR RT-DERAT 55/5004, Paris, 1989.

[13]Gendre, P., "Experimental Results on A-Airfoil Geometry," CERFACS, TR, Toulouse, France, 1990.

[14]Shur, M., Spalart, P., Strelets, M., and Travin, A., "Detached-Eddy Simulation of an Airfoil at High Angle of Attack," *Engineering Turbulence Modelling and Experiments*, edited by W. Rodi and D. Laurence, Vol. 4, Elsevier, New York, 1999, pp. 669–678.

[15]Werner, H., and Wengle, H., "Large-Eddy Simulation of Turbulent Flow Over and Around a Cube in a Plane Channel," *Selected Papers from the 8th Symposium on Turbulent Shear Flows*, edited by F. Durst, R. Friedrich, B. Launder, F. Schmidt, U. Schumann, and J. Whitelaw, Springer, Berlin, 1993, pp. 155–168.

[16]Choi, H., and Moin, P., "Effects of the Computational Time Step on Numerical Solutions of Turbulent Flows," *Journal of Computational Physics*, Vol. 113, No. 1, 1994, pp. 1–4.

[17]Germano, M., Piomelli, U., Moin, P., and Cabot, W., "A Dynamic Subgrid-Scale Eddy Viscosity Model," *Physics of Fluids A*, Vol. 3, No. 7, 1991, pp. 1760–1765.

[18]Lilly, D., "A Proposed Modification of the Germano Subgrid-Scale Closure Method," *Physics of Fluids A*, Vol. 4, No. 3, 1992, pp. 633–635.

[19]Ducros, F., Nicoud, F., and Poinsot, T., "Wall-Adapting Local Eddy-Viscosity Models for Simulations in Complex Geometries," *Numerical Methods for Fluid Dynamics VI*, edited by M. J. Baines, Oxford Univ. Computing Lab., Oxford, 1998, pp. 293–299.

[20]Lenormand, E., Sagaut, P., Phuoc, L. T., and Comte, P., "Subgrid-Scale Models for Large-Eddy Simulation," *AIAA Journal*, Vol. 38, No. 8, 2000, pp. 1340–1350.

[21]Spalart, P., and Allmaras, S., "A One-Equation Turbulence Model for Aerodynamic Flows," *La Recherche Aérospatiale*, Vol. 1, 1994, pp. 5–21.

[22]Mary, I., and Sagaut, P., "Large Eddy Simulation of Flow Around a High Lift Airfoil," *Proceedings of Direct and Large Eddy Simulation Workshop 4*, edited by B. Geurts, R. Friedrich, and O. Métais, 2001, Kluwer, Dordrecht, The Netherlands, pp. 95–98.

[23]Spalart, P., "Young Person's Guide to Detached Eddy Simulation Grids," NASA CR-2001-211032, NASA Langley Research Center, July 2001.

[24]Weber, C., and Ducros, F., "Large-Eddy and Reynolds Averaged Navier–Stokes Simulations of Turbulent Flow Over an Airfoil," *International Journal of Computational Fluid Dynamics*, Vol. 13, No. 4, 2000, pp. 327–355.

[25]Schmidt, S., and Thiele, F., "Detached Eddy Simulation of Flow Around A-Airfoil," *Proceedings of IUTAM Symposium, Unsteady Separated Flows*, [CD-ROM], edited by M. Braza, C. Hirsch, and F. Hussain, Institut de Méchanique des Fluides, Toulouse, France, 2002.

[26]Schmidt, S., and Thiele, F., "Detached and Large-Eddy Simulation of a NACA 4412 Airfoil Flow with Semi-Structured Grids," *LES of Complex Transitional and Turbulent Flows, Proceedings of EUROMECH Colloquium 412*, edited by R. Friedrich and W. Rodi, Kluwer, Dordrecht, The Netherlands, 2002, pp. 255–272.

[27]Fröhlich, J., and Mellen, C., "Transition in LES of Bluff Body Flows and Airfoils," *Direct and Large-Eddy Simulation*, edited by B. Geurts, R. Friedrich, and O. Metais, Vol. 4, Kluwer Academic, Norwell, MA, 2001, pp. 145–156.

P. Givi
Associate Editor